Small-angle X-ray Scattering from Multi-walled Carbon Nanotubes (CNTs) Dispersed in Polymeric Matrix

Toru Inada, Hiroyasu Masunaga, Shinichi Kawasaki,† Masahiro Yamada,† Kana Kobori,† and Kazuo Sakurai*
Department of Chemical Process & Environments, Faculty of Environmental Engineering, The University of Kitakyushu, 1-1, Hibikino, Wakamatu-ku, Kitakyushu 808-0135
†*Advanced Material Business Promotion Department, Osaka Gas Co., Ltd., 6-19-9, Torishima Konohana-ku, Osaka, 554-0051*

(Received January 24, 2005; CL-050111)

Small-angle X-ray scattering (SAXS) was measured from CNT-dispersed resins and the data was analyzed in terms of a core-shell cylinder model. The structural parameters obtained from SAXS perfectly agreed with those from the electron microscopic observations. However, we found that SAXS was rather insensitive to how CNTs were dispersed in the resins.

Discovery of carbon nanotubes (CNTs) seems to have broadened our horizon in the technology of polymeric composites, because of the novel mechanical properties of CNTs. Their high strength and stiffness, and the enormously large aspect ratio exhibit a high potential for an excellent filler for the composites. In fact, experimental trials to prepare a CNT-dispersed resin have been made and some of the preliminary results have shown improved mechanical properties,[1] and an electrical and thermal conductivity together with a low density.[2] However, CNTs are inherently cohesive because of both π–π and van der Waals attractions. This nature makes it extremely difficult for CNTs to be handled industrially as well as experimentally. The better understanding how CNTs are dispersed in polymeric matrix should give the more improvement of the physical properties. Although not from a CNT-dispersed resin, Yurekli et al.[3] first carried out small-angle neutron scattering from a single-walled CNT dispersed in a water/surfactant system. Their data can be interpreted by dispersed CNTs that has randomly adsorbed surfactants on the CNT surface, rather than by the previously hypothesized formation of cylindrical micelles with the CNTs forming the core of cylinders. Their system contained both the micelles made from only the surfactants and the dispersed CNTs with the surfactants. Therefore, it seemed difficult to isolate the scattering from CNT itself from others. In this paper, we dispersed multiwalled CNTs in a polymer solution with a vibratory ball mill and spin-casted the resultant solution on a glass surface to obtain a CNTs-dispersed film. We used four resins which have been widely used in wet-coating; polystyrene, polycarbonate,[4] fluorene-containing polyester (FBP),[5] and bisphenol Z polycarbonate (PC-Z).[4] We carried out small- and wide-angle synchrotron X-ray scattering from the films as well as conductivity measurements, aiming to interpolate the scattering with dispersed CNTs in the resins.

Figure 1a presents a representative TEM image for the CNT samples used in this work, showing a typical feature for multiwalled CNTs, namely, a hollow tubular architecture with a diameter of 20–25 nm and a shell thickness of 4–6 nm. We prepared most of the films with a resin/CNT ratio of 3:1 (in weight), because we found that there was essentially no resin/CNT ratio dependence of the observed scattering. With increasing the mill-crashing time, it seemed that CNTs were cut short or the structure was crashed.[6] In fact, we found that the film conductivity decreased with increasing the crashing time, although the scattering profiles did not change so much. Figures 1b and 1c compare the optical microscopic images for the casted film surface between FBP and PC-Z. Although both films were prepared with the same method, seemingly CNTs were more uniformly dispersed in FBP than in PC-Z. Difference in the dispersion ability is more clearly demonstrated with SEM observation. According to Sakurai et al.,[7] FBP has shown better solubility than other conventional polymers, such as bisphenol A polycarbonate and polyethylene terephthalate. The exact molecular mechanism for the large difference in dispersion has been still under investigation, however, we suppose that there is a specific interaction between the fluorene moiety and the aromatic compound, such as π–π interactions.

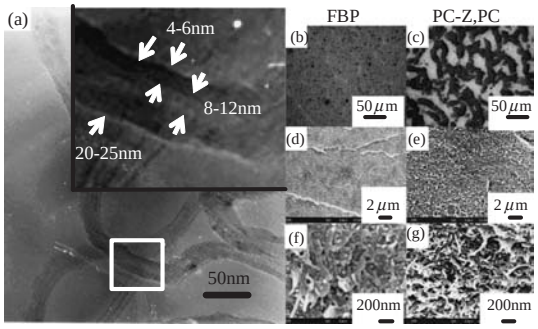

Figure 1. TEM images for the CNT used in this paper (a), and comparison of optical microscopic images between PC-Z/CNT and FBP/CNT composites (b) and (c), and corresponding SEM images (d)–(g). The inset of (a) is the magnified image of the CNT part marked by the rectangular.

Figure 2 plot the SAXS intensities [$I(q)$] from a CNT-dispersed FBP film against the magnitude of the scattering vector (q), comparing with the calculated $I(q)$ for a core-shell or hard cylinder model with a radius of 10 nm. If the cylinder length is sufficiently large, $I(q)$ from a core-shell cylinder can be expressed as follows;

$$I(q) \propto \frac{1}{q}\left\{V_{\text{core}}(\rho_{\text{C}} - \rho_{\text{S}})\frac{1}{qR_{\text{C}}}J_1(qR_{\text{C}}) + V_{\text{shell}}\rho_{\text{S}}\frac{1}{qR_{\text{S}}}J_1(qR_{\text{S}})\right\}^2 \quad (1)$$

where, R_{C} and R_{S} are the radii of the core and shell of the core-shell cylinder. V_{core} and V_{shell} are the volumes of the core and shell parts, $J_1(x)$ is the first order Bessel function, and ρ_{C} and ρ_{S} are the electron densities of the core and shell, respectively.

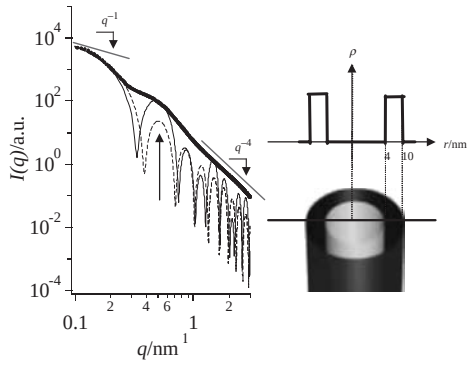

Figure 2. SAXS profile from a FBP/CNT composite with a filler/resin weight ratio of 1/3 (○), comparing with the theoretical calculations for a core-shell (straight line) and hard cylinder models (dotted line). The best fit parameters are schematically illustrated in the inset.

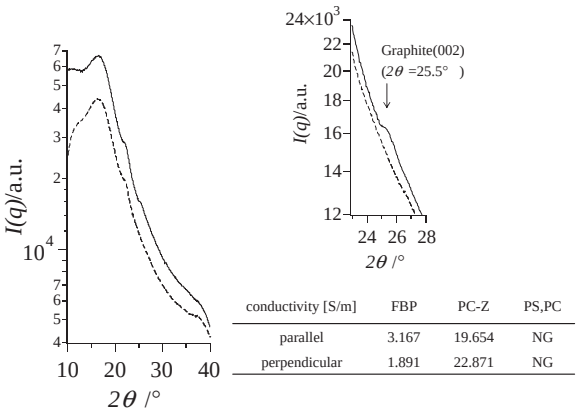

conductivity [S/m]	FBP	PC-Z	PS,PC
parallel	3.167	19.654	NG
perpendicular	1.891	22.871	NG

Figure 3. Comparison of WAXS profiles between parallel (dotted line) and perpendicular (straight line) to the casting directions and corresponding conductivities.

Since we found that the infinite cylinder model (rather than finite cylinders) was enough to interpolate the data, we used Eq 1 to calculate the theoretical values in Figure 1. For simplicity, we assumed $\rho_C = 0$ in the calculation. When the scatterers are cylindrical, $I(q)$ obeys the characteristic relation of $I(q) \propto q^{-1}$ in the range of $2\pi/L < q < 1/R$, where L and R are the length and radius of a cylinder equivalent to the scatterer.

By comparing the q^{-1} line drawn in the figure, it can be seen that the obtained data show an asymptotic behavior reaching this characteristic slope in the lower q region. When we superimpose the data with a theoretical line in the lower q region ($q < 0.3\,\mathrm{nm}^{-1}$, denoted by the first oscillation) as presented in the figure, any hard cylinder model can not fit the data in the range of $q > 0.5\,\mathrm{nm}^{-1}$, failing to reproduce the intensity for the second oscillation and the decay of the higher q regime. In order to fit the data for $q > 0.5\,\mathrm{nm}^{-1}$, we had to assume a core-shell model with a shell thickness of 6 nm. As presented in the supplemental information, the shell thickness sensitively determines the intensity and position of the second oscillation. As shown in the figure, the combination of $R_C = 4$ and $R_S = 6$ nm can almost completely fit the experimental data, and more importantly, these values agree with TEM observation. The intensity decays in a manner of $I(q) \propto q^{-4}$ in the higher q regime predicted by the Porod low. This feature is consistent with that the CNT-resin interface seemed be very sharp.

There was no significant difference in the SAXS data among the different four resins, except for the low angle region. For the PC-Z and PS systems, $I(q)$ vs q plots went downward in the range of $q < 0.15\,\mathrm{nm}^{-1}$. Although, we need a measurement at the lower angle, these features can be ascribed to aggregation of CNTs. Except for the low angle behaviors, the SAXS data did not depend on neither the crashing time, the CNT concentration, nor resins.

Figure 3 compares WAXS patterns between parallel and perpendicular to the casting directions for the CNT-dispersed FBP as well as the conductivity measurements. The difference in the conductivity between the two directions is only 1.7 times and the WAXS peak corresponding to the graphite (002) diffraction does not show significant difference. The perpendicular profile seems to have a larger (002) diffraction than the parallel one, however, there was no obvious intensity maximum observed at the perpendicular direction. The (002) diffraction was rather spread around this direction. These results show that the simple casting is not enough to orient the CNT fibers. Gojny et al.[8] added a carbon black to their CNT/resin composite to increase the conductivity. The idea is that the addition of carbon blacks eliminates (or reduce) the contact resistance. When we added a carbon black to our system, although the conductivity was increased, the anisotropy was not improved. As presented in the table, PC-Z/CNT shows a larger conductivity than that of FBP/CNT, suggesting that CNT is better dispersed in PC-Z than in FBP. However, this conclusion contradicts to that from the optical and SEM observation. Furthermore, SAXS seem insensitive to how CNTs are dispersed in resins. We are in the process of investigating these unclear results.

To sum up, SAXS from a CNT-dispersed resin exhibits the profiles which can be interpreted with a core-shell cylinder and the structural parameters agreed with those obtained from electron microscopy.

TEM and SEM were performed at the analytical center at Kitakyushu University and SAXS and WAXS, at SPring-8 BL40B2 (2004A0425-NL2b-np and 2004B0135-NL2b-np). This work is finically supported by a Grant-in-Aid for Scientific Research (Nos. 16350068 and 16655048).

References

1 T. Liu, I. Y. Phang, L. Shen, S. Y. Chow, and W. D. Zhang, *Macromolecules*, **37**, 7214 (2004).
2 D. T. Colbert, "Plastics, Additives and Compounding," (2003), Vol. 5, Issue 1, pp 18–25.
3 K. Yurekli, C. A. Mitchell, and R. Krishnamoorti, *J. Am. Chem. Soc.*, **126**, 9902 (2004).
4 M. Kawai, A. Toriumi, M. Nozomi, O. Murakami, K. Fujioka, and R. E. Cais, IS&T's Tenth International Congress on Advances in Non-Impact Printing Technologies (1994), p 265.
5 K. Yao, M. Koike, Y. Suzuki, K. Sakurai, T. Indo, and K. Igarashi, U. S. Patent 6,255,031 (2001).
6 H. Takase, Y. Mikata, S. Matsuda, A. Murakami, in "Seikei-Kakou," the Japan Society of Polymer Processing, Japan (2002), Vol. 14, No. 2, pp 126–131.
7 K. Sakurai and M. Fuji, *Polym. J.*, **32**, 676 (2000).
8 F. H. Gojny, M. H. G. Wichmann, U. Kopke, B. Fiedler, and K. Schulte, *Compos. Sci. Technol.*, **64**, 2363 (2004).

Published on the web (Advance View) March 5, 2005; DOI 10.1246/cl.2005.524